Simple Analytical Solution to Electromagnetic Scattering by Two-Dimensional Conducting Object with Edges and Corners: Part I—TM Polarization

Korada Umashankar, *Senior Member, IEEE*, Wan Chun, *Student Member, IEEE*, and Allen Taflove, *Fellow, IEEE*

Abstract—**A simple and approximate analytical solution is presented by invoking on-surface radiation condition (OSRC) theory for the analysis of electromagnetic scattering by a perfectly conducting two-dimensional object. The scattering object is assumed to be placed in a free space medium and is excited by a time harmonic plane wave having transverse magnetic (TM) polarization. The closed form analytical result for the monostatic as well as bistatic radar cross section is approximate and is useful in many engineering studies. It is applicable only for the case of a convex shaped conducting object having arbitrary two dimensional cross section with arbitrary edges and corners. Canonical scattering objects, such as a triangular shaped scatterer and a thin strip scatterer are analyzed for the transverse magnetic excitation to evaluate usefulness of the analytical results reported in this paper. Numerical data for the monostatic as well as the bistatic radar cross section are also presented by comparing them with respect to the numerical solution obtained by solving an electric field integral equation based on the method of moments technique.**

I. Introduction

THERE exist numerous analytical and numerical approaches for analyzing the electromagnetic scattering by a perfectly conducting object [1]–[7]. Generally, the formulation of the scattering problem is accomplished in terms of either a differential equation or an integral equation by treating it as a boundary value problem. The analytical approach is limited in its application to canonical objects, and for analyzing practical scattering geometries the numerical approaches based on the matrix method [3], the finite element or the finite difference method [7] are widely used. Even though many analytical and numerical methods are widely reported [2], [7] in the literature for various class of material and scattering geometries, still in many engineering applications involving electromagnetic scattering studies, there exists a need for simple analytical tools for the induced electric current and the corresponding radar cross section of arbitrary shaped conducting object. The purpose of this paper is to report a possible approach to obtain simple and approximate solution (yet form an useful tool for many engineering applications) of the electromagnetic scattering by a perfectly conducting object having arbitrary edges and corners. The study reported in the following section is limited to the two-dimensional scattering object placed in a free space medium which is excited by a time harmonic plane wave having transverse magnetic (TM) polarization. The analysis is accomplished by invoking the on-surface radiation condition (OSRC) theory [8]. It can be noted that the OSRC approach basically utilizes an additional boundary relationship for the normal derivative of the scattered electric field which is proportional to the scattered magnetic field by implementing, in a limit, a higher order near field radiation boundary condition [9], [10] directly on the surface of scattering object. In fact, for the study of scattering by two-dimensional convex conducting object, the OSRC has exposed [11], [14] substantial simplification of the usual integral equation for the induced surface electric current distribution, and it is interesting to note that elaborate numerical approaches are no longer required.

A preliminary OSRC study using the first- and second-order operators is reported in [8] for the electromagnetic scattering by a two-dimensional circular conducting scatterer for TM and transverse electric (TE) plane wave excitations. The validation data for the induced surface current and the bistatic radar cross section with the application of second-order OSRC operator show agreement in the illuminated region for both the TM and TE excitations. But the results are inconclusive with respect to very low level field distribution in the deep shadow region for the TM excitation, and similarly, are inconclusive to predict creeping wave fields deep in the shadow region for the TE excitation. In fact, using the third and fourth higher order OSRC operators a detailed study is assessed in [14] for the OSRC analysis of scattering by a circular conducting object for both TM and TE excitations. Even though a third- or a fourth-order differential equation is to be solved for the application of higher order OSRC operators, the investigation [14] predicts the distribution of

Manuscript received January 10, 1990; revised August 12, 1991. This work was supported in part by Office of Naval Research (ONR) grant N00014-88-K-0475 and by National Science Foundation (NSF) Grant ASC-8811273.

K. Umashankar and W. Chun are with the Department of Electrical Engineering and Computer Science, University of Illinois, Chicago, IL 60680.

A. Taflove is with the Department of Electrical Engineering and Computer Science, McCormick School of Engineering, Northwestern University, Evanston, IL 60208.

IEEE Log Number 9104567.

low level fields with the TM excitation, and similarly, predicts behavior of creeping wave fields deep in the shadow region with the TE excitation. In a separate study, the application of second-order OSRC is also extended for the analysis of electromagnetic scattering and penetration by a homogeneous convex dielectric object [11], [12]. Further, in the OSRC study reported in [8] for the cases of thin strip and square scatterer, the dominant effect of the singular electric currents at the geometric corners are not considered, but only the physical optics type currents are taken into account in the calculation of radar cross section.

For considering application to engineering oriented problems, this paper presents a simple and approximate analysis to include the additional effects due to radiation from the sharp corners [4], [6], [14] so that arbitrary cross-sectional convex geometries consisting of arbitrary edges and corners can be systematically analyzed. For the scattering geometries considered, it is shown that the second-order OSRC result for the induced electric current has a some relevance to the electric currents of the physical theory of diffraction. Two canonical conducting objects, such as a triangular shaped scatterer and a thin strip scatterer are analyzed for the plane wave excitation with TM polarization to evaluate the simple and approximate analytical results reported in this paper. Comparative data for the monostatic as well as the bistatic radar cross section are also presented by comparing the second-order OSRC results with respect to the numerical solution obtained by solving the electric field integral equation based on the method of moments technique [3]. Similar analytical study [14] can also be considered for a plane wave excitation with TE polarization, and is reported separately.

II. Formulation—TM Polarization

Let us consider a two-dimensional, convex, conducting scatterer having an arbitrary cross section with arbitrary edges and corners. It is excited normally by a TM polarized plane wave as shown in Fig. 1. The scatterer is assumed to be uniform in z coordinate direction and the various electric and magnetic field quantities are independent of the z coordinate variation. The cross section of the arbitrary conducting scatterer is contained in region 2 and is bounded by a contour C_s. Outside region 2 is region 1 representing an isotropic free space medium. Referring to Fig. 1, let

$(E_z^s, \bar{H}^s)$: scattered electric and magnetic fields in region 1
$(E_z^i, \bar{H}^i)$: incident electric and magnetic fields in region 1.

For the TM polarized excitation, the z component of the incident plane wave electric field can be written as

$$E_z^i(\rho, \phi) = E_0 e^{-jk\rho\cos(\phi - \phi^i)} \tag{1}$$

where

k: propagation constant of the free space medium
ϕ^i: incident angle of the exciting TM plane wave.

Further, the z component of scattered electric field [1], [2] in the regions 1 is obtained by

$$E_z^s(\bar{\rho}) = \oint_{C_s} \left[\mathcal{S}(\bar{\rho}, \bar{\rho}') + \mathcal{J}(\bar{\rho}, \bar{\rho}') \right] ds' \tag{2a}$$

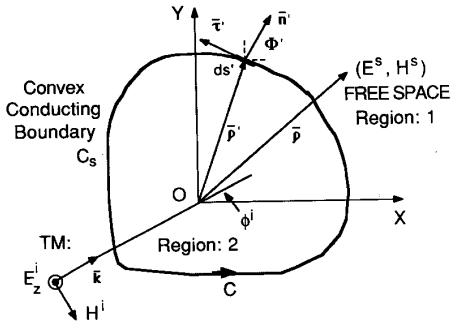

Fig. 1. Two-dimensional arbitrary shaped convex conducting scatterer—TM excitation.

$$\mathcal{S}(\bar{\rho}, \bar{\rho}') = G(\bar{\rho}, \bar{\rho}') \frac{\partial E_z^s(\bar{\rho}')}{\partial n'} \tag{2b}$$

$$\mathcal{J}(\bar{\rho}, \bar{\rho}') = -E_z^s(\bar{\rho}') \frac{\partial G(\bar{\rho}, \bar{\rho}')}{\partial n'} \tag{2c}$$

where the two-dimensional Green's function

$$G(\bar{\rho}, \bar{\rho}') = \frac{1}{4j} H_0^{(2)}(k\,|\,\bar{\rho} - \bar{\rho}'\,|). \tag{2d}$$

$H_0^{(2)}$ is the Hankel function of second kind and zero order

On the scatterer boundary contour C_s, n' and s' represent the normal and the tangential variables along the corresponding unit vectors given by

$$\hat{n}' = \hat{x}'\cos\Phi' + \hat{y}'\sin\Phi' \tag{3a}$$

$$\hat{s}' = -\hat{x}'\sin\Phi' + \hat{y}'\cos\Phi'. \tag{3b}$$

Φ' is the angle of the normal unit vector with respect to x coordinate axis

On referring to (2a), the scattered electric field at any point outside the conducting scatterer can be calculated, if the scattered electric field and the normal derivative of the scattered electric field are known along the boundary contour C_s. To determine these two unknown field quantities, the following two near-field boundary relationships are utilized. The relationship for the scattered electric field is obtained by enforcing the regular conducting boundary condition that the tangential z component of the total electric field is equal to zero on the boundary contour C_s

$$E_z^s(\bar{\rho}') = -E_z^i(\bar{\rho}'), \qquad \bar{\rho}' \text{ on } C_s. \tag{4}$$

The relationship for the normal derivative of scattered electric field is obtained by (invoking directly on the boundary contour C_s) the second-order on-surface radiation boundary condition [8], [10], [14] for the outgoing scattered cylindrical waves. According to the OSRC approach [8], the axial component of the scattered electric field at a radial distance ρ should satisfy the following outgoing radiation boundary condition in terms of radial coordinate variables

$$\mathcal{B}_2 E_z^s = -\frac{1}{\rho^2}\frac{\partial^2}{\partial\phi^2}E_z^s + \left[2jk + \frac{2}{\rho}\right]\frac{\partial}{\partial\rho}E_z^s + \left[-2k^2 + \frac{3jk}{\rho} + \frac{3}{4\rho^2}\right]E_z^s \approx O(\rho^{-9/2}). \tag{5a}$$

The above second-order OSRC boundary operator yields a relationship for the normal derivative of scattered electric field on the conducting scatterer and is given by

$$\frac{\partial E_z^s(\bar{\rho}')}{\partial n'} = \left[\frac{\xi(s')}{2} + jk + \frac{j\xi^2(s')}{8[k - j\xi(s')]}\right] E_z^i(\bar{\rho}') + \frac{j}{2[k - j\xi(s')]} \frac{\partial^2 E_z^i(\bar{\rho}')}{\partial s'^2}. \quad (5b)$$

$\xi(s')$ is the curvature of the osculating circle at location s' on contour C_s

$$\frac{\partial^2 E_z^i(\bar{\rho}')}{\partial s'^2} = -k^2[\sin^2\Phi'\cos^2\phi^i + \cos^2\Phi'\sin^2\phi^i - 2\sin\Phi'\cos\Phi'\cos\phi^i\sin\phi^i] E_z^i(\bar{\rho}'). \quad (5c)$$

The two boundary conditions (4) and (5b) for the scattered electric field and its normal derivative on the contour C_s are now substituted into expressions (2b) and (2c), and the scattered electric near-field distribution in region 1, expression (2a), can be calculated for a given arbitrary boundary contour C_s. Further, for the case of TM excitation, the z directed induced electric current on the conducting scatterer is directly proportional to the normal derivative of the total electric field and is given by

$$J_z(\bar{\rho}') = \frac{-j}{\eta k}\left[\frac{\partial E_z^s(\bar{\rho}')}{\partial n'} + \frac{\partial E_z^i(\bar{\rho}')}{\partial n'}\right] \quad (6)$$

where η is the intrinsic impedance of region 1. The far-field distribution can also be derived using the expression (2a) with the two-dimensional Green's function term (2d) replaced with its large argument approximation.

III. Conducting Triangular Scatterer

To illustrate a procedure to analyze an arbitrary convex conducting scatterer with edges and corners, and to obtain a simple analytical solution by performing the integration along the close boundary contour C_s, a triangular scattering geometry of Fig. 2, with three straight edges and three wedge type corners is considered. At the sharp corners, there exists a geometrical discontinuity and thus the curvature of the osculating circle for the corner region is undefined. In order to overcome this difficulty, the sharp corners of the scattering geometry are rounded off [13], [14] by smooth contours, for example, small circular regions are inserted with a limiting radius ϵ and centered at the corners. A virtual boundary contour C_v is now drawn enclosing the conducting scatterer such that it is always parallel to the original boundary contour C_s and is also drawn tangential to each of the small limiting circles located at the geometrical sharp corners as shown in Fig. 2. In a limit as the radius ϵ tends to zero, the virtual boundary contour C_v exactly coincides with the original boundary contour C_s of the conducting scattering object. On referring to expression (2) and Fig. 2, the z component of scattered electric field at any point in the region 1 is given by

$$E_z^s(\bar{\rho}) = \lim_{\epsilon\to 0} \oint_{C_v} \left[\mathcal{S}(\bar{\rho}, \bar{\rho}') + \mathcal{J}(\bar{\rho}, \bar{\rho}')\right] ds'. \quad (7)$$

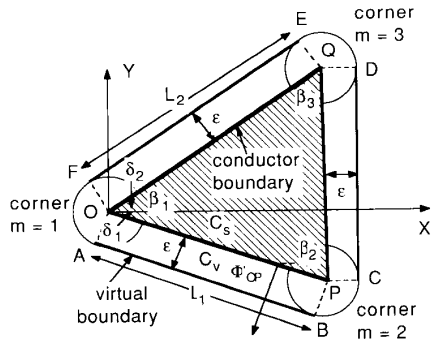

Fig. 2. Geometry of triangular conducting scatterer—TM excitation.

C_v are contour segments FA + AB + BC + CD + DE + EF where the virtual contour C_v enclosing the triangular scatterer, is split into six segments. The terms in integrand of the integral expression (7) are completely known in terms of the geometrical parameters of the scattering object and the plane wave incident field. Since the radius of the limiting circle located around the corners, $m = 1$, 2, and 3, is very small and in a limit tends to zero, it is assumed that the integrand of (7) does not vary along the arc length of the limiting circle. Hence, the integral expression for the scattered electric field distribution in region 1 simplifies to the sum of two specific terms consisting of the three smooth edge contributions and the three corner contributions with explicit dependence on the angle of incidence of TM plane wave excitation, and is given by

$$E_z^s(\bar{\rho}) = \left[\int_{OP} + \int_{PQ} + \int_{QO}\right]\left[\mathcal{S}(\bar{\rho}, \bar{\rho}') + \mathcal{J}(\bar{\rho}, \bar{\rho}')\right] ds' + \sum_{m=1}^{3} \frac{3E_0}{32j}(\pi - \beta_m) H_0^{(2)} \cdot (k\,|\,\bar{\rho} - \bar{\rho}'_m\,|) e^{-jk\rho'_m\cos(\phi'_m - \phi^i)}. \quad (8)$$

By taking the large argument approximation for the Green's function (2d), expression (8) can be conveniently simplified to obtain an analytical solution for the scattered electric far field distribution. Hence, in the far-field region, (8) yields

$$E_z^s(\rho, \phi) \sim \frac{e^{-j\pi/4}}{\sqrt{8\pi k}}\left[A_0 + \sum_{m=1}^{3} C_m\right] E_0 \frac{e^{-jk\rho}}{\sqrt{\rho}} \quad (9a)$$

$$A_0 = \left[\int_{OP} + \int_{PQ} + \int_{QO}\right] \cdot \left[\frac{\partial E_z^s(\bar{\rho}')}{\partial n'} + jk\cos(\phi - \Phi') E_z^i(\bar{\rho}')\right] \cdot e^{jk\rho'\cos(\phi - \phi')}\, ds' \quad (9b)$$

$$= jk\{T_{OP} + \cos(\phi - \Phi'_{OP})\}\left[\frac{e^{j\gamma_{OP}L_1} - 1}{j\gamma_{OP}}\right] + jk\{T_{PQ} + \cos(\phi - \Phi'_{PQ})\} \cdot \left[\frac{e^{j\gamma_{PQ}L_2\sin\delta_2} - e^{-j\gamma_{PQ}L_1\sin\delta_1}}{j\gamma_{PQ}}\right] e^{j\alpha_{PQ}L_1}$$

$$+ jk\{T_{QO} + \cos(\phi - \Phi'_{QO})\} \cdot \left[\frac{1 - e^{-j\gamma_{QO}L_2}}{j\gamma_{QO}}\right] \quad (9c)$$

and

$$C_m = \frac{3}{8}(\pi - \beta_m) e^{-jk\rho'_m[\cos(\phi'_m - \phi^i) - \cos(\phi'_m - \phi)]} \quad (9d)$$

where the various angular terms are given by

$$T_{OP} = 1 - \frac{1}{2}\{\sin^2\Phi'_{OP}\cos^2\phi^i + \cos^2\Phi'_{OP}\sin^2\phi^i - 2\sin\Phi'_{OP}\cos\Phi'_{OP}\cos\phi^i\sin\phi^i\} \quad (10a)$$

$$\gamma_{OP} = k[-\cos(\phi'_{OP} - \phi^i) + \cos(\phi'_{OP} - \phi)] \quad (10b)$$

$$T_{PQ} = 1 - \frac{1}{2}\sin^2\phi^i \quad (11a)$$

$$\gamma_{PQ} = k[-\sin\phi^i + \sin\phi] \quad (11b)$$

$$\alpha_{PQ} = k[-\cos\phi^i + \cos\phi]\cos\delta_1 \quad (11c)$$

$$T_{QO} = 1 - \frac{1}{2}\{\sin^2\Phi'_{QO}\cos^2\phi^i + \cos^2\Phi'_{QO}\sin^2\phi^i - 2\sin\Phi'_{QO}\cos\Phi'_{QO}\cos\phi^i\sin\phi^i\} \quad (12a)$$

$$\gamma_{QO} = k[\cos(\phi'_{QO} - \phi^i) - \cos(\phi'_{QO} - \phi)]. \quad (12b)$$

The radar cross section of the conducting triangular scatterer can now be calculated using the far-field expression (9a)

$$\text{RCS} = \lim_{\rho\to\infty} 2\pi\rho\left|\frac{E_z^s(\phi)}{E_z^i(\phi)}\right|^2. \quad (13)$$

Similar to the treatment in physical theory of diffraction [4], [6], the scattered electric field distribution can be viewed as the contribution from the induced electric currents on the triangular shaped conducting scatterer. It consists of the contribution due to currents on the three smooth edges and the localized currents due to the three corner effects. As can be seen, the distribution of the electric current due to corner effects is only approximate. In the context of presenting a simple and an approximate analytical solution, the corner effects are considered only due to the dominant curvature effect, but the remaining minor contribution [15] due to slope of the radius of curvature is excluded. The z directed induced electric current distribution at any point along the triangular edge OP is given by

$$J_z(\bar{\rho}') = J_z(\bar{\rho}')\,|_{\text{edge effect}} + J_z(\bar{\rho}')\,|_{\text{corners}}, \qquad \bar{\rho}' \text{ on } OP. \quad (14a)$$

Using (1), (5b), and (6), the electric current due to edge effect is given by

$$J_z(\bar{\rho}')\,|_{\text{edge } OP} = \frac{-j}{\eta k}\left[\frac{\partial E_z^s(\bar{\rho}')}{\partial n'} + \frac{\partial E_z^i(\bar{\rho}')}{\partial n'}\right], \qquad \bar{\rho}' \text{ on } OP \quad (14b)$$

$$= \frac{1}{\eta}\left[1 - \frac{1}{2}\{\sin^2\Phi'_{OP}\cos^2\phi^i + \cos^2\Phi'_{OP}\sin^2\phi^i - 2\sin\Phi'_{OP}\cos\Phi'_{OP}\cos\phi^i\sin\phi^i\} - \cos(\Phi'_{OP} - \phi^i)\right] E_z^i(\bar{\rho}'_{OP}). \quad (14c)$$

Further, in (8), the scattered electric field distribution due to the three wedge type corners can be viewed as the contribution due to the localized electric current distributions which principally exist at the three corners $m = 1$, 2, and 3 of the scatterer in the form of isolated line sources with weighted amplitudes corresponding to the internal wedge angle β_m and the angle of TM incident excitation.

Based on (9a) and (13), Fig. 3(a) shows the monostatic radar cross section in decibels for the case of a perfectly conducting triangular scatterer as a function of monostatic angle $\phi = \pi + \phi^i$. For the triangular scatterer, the dimensions are selected as $kL_1 = kL_2 = 10$ and the angle $\beta_1 = \pi/3$ which corresponds to an equilateral triangular scatterer. The OSRC result for the radar cross section shown in Fig. 3(a) is also compared with an alternative numerical solution obtained based on the electric field integral equation [3] for a two-dimensional conducting scatterer. The electric field integral equation is solved using the method of moments numerical scheme with a resolution of 20 pulse samples for every half-wavelength. Two types of monostatic comparison data are presented in Fig. 3(a). If the three corner effects are excluded, the comparison between OSRC and integral equation monostatic data is poor for certain incident angles. With the three corner effects included, a better comparison is obtained for various excitation angles including broadside and grazing angles of incidence. Similarly, Fig. 3(b) shows comparative result for the bistatic radar cross section in decibels for the same triangular scatterer with broad side excitation on one edge.

IV. Conducting Thin Strip Scatterer

In order to illustrate further the application of the integral expression (7) and to obtain a simple analytical solution by performing the integration along the close boundary contour C_s, a thin strip scattering geometry of Fig. 4 with one straight edge and two corners is considered. Again, the two sharp corners of the thin strip scattering geometry are rounded off [13], [14] by inserting small circular regions with a limiting radius ϵ and centered at the corners. A virtual boundary contour C_v is now drawn enclosing the thin strip scatterer such that it is always parallel to the original boundary contour C_s and is also drawn tangential to each of the small limiting circles. Referring to the Fig. 4, in a limit as the radius ϵ tends to zero, the virtual boundary contour C_v exactly coincides with the original boundary contour C_s of the scattering object. Now, the axial component of scattered electric field at any point in region 1 is given by

$$E_z^s(\bar{\rho}) = \lim_{\epsilon\to 0}\oint_{C_v}\left[\mathcal{S}(\bar{\rho}, \bar{\rho}') + \mathcal{J}(\bar{\rho}, \bar{\rho}')\right] ds'. \quad (15)$$

C_v are contour segments $DA + AB + BC + CD$ and where the virtual contour C_v enclosing the thin strip scatterer, is

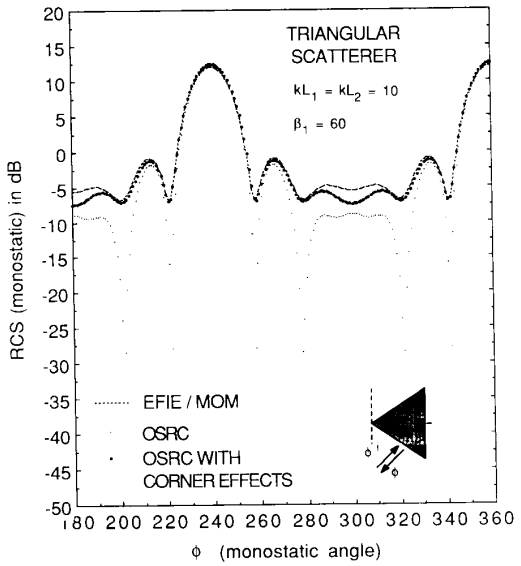

(a)

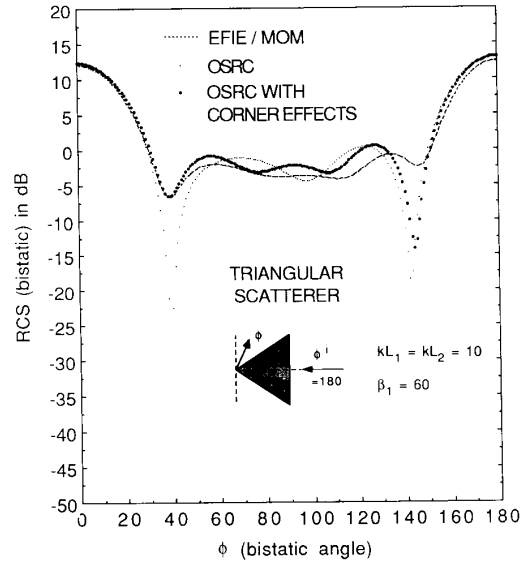

(b)

Fig. 3. Monostatic radar cross section of triangular conducting scatterer using second-order OSRC—TM excitation. (b) Bistatic radar cross section of triangular conducting scatterer using second-order OSRC—TM excitation, $\phi^i = 180$.

split into four segments. The terms in integrand of the integral expression (15) are completely known in terms of the geometrical parameters of the thin strip and the plane wave incident field. Since the radius of the limiting circle located around a corner is very small and in a limit tends to zero, again it is assumed that the integrands of (15) do not vary along the arc length of the limiting circle. Hence, the integral expression for the scattered electric field distribution in region 1 simplifies to the sum of two specific terms consisting of the smooth edge contribution and the two corner contributions, $m = 1$ and 2, and is given by

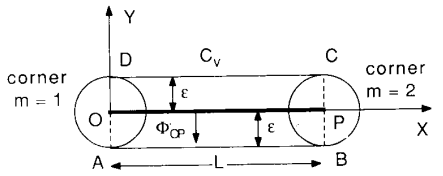

Fig. 4. Geometry of thin strip conducting scatterer—TM excitation.

$$E_z^s(\bar{\rho}) = \left[\int_{OP} + \int_{PO}\right]\left[\mathcal{S}(\bar{\rho}, \bar{\rho}') + \mathcal{J}(\bar{\rho}, \bar{\rho}')\right] ds' + \frac{3E_0}{32j}\pi H_0^{(2)}(k\rho) + \frac{3E_0}{32j}\pi H_0^{(2)}(k\,|\,\bar{\rho} - \bar{\rho}_2'\,|)e^{-jkL\cos\phi^i}. \quad (16)$$

By taking the large argument approximation for the Green's function (2d), (16) can be conveniently simplified to obtain an analytical solution for the scattered electric far field distribution. Hence, in the far-field region, (16) yields

$$E_z^s(\rho, \phi) \sim \frac{e^{-j\pi/4}}{\sqrt{8\pi k}}\left[A_0 + C_1 + C_2\right]E_0\frac{e^{-jk\rho}}{\sqrt{\rho}} \quad (17a)$$

$$A_0 = \left[\int_{OP} + \int_{PO}\right] \cdot \left[\frac{\partial E_z^s(\bar{\rho}')}{\partial n'} + jk\cos(\phi - \Phi')E_z^i(\bar{\rho}')\right] \cdot e^{jk\rho'\cos(\phi - \phi')}\, ds' \quad (17b)$$

$$= jk\{T_{OP} - \sin\phi\}\left[\frac{e^{j\gamma_{OP}L} - 1}{j\gamma_{OP}}\right] + jk\{T_{PO} + \sin\phi\}\left[\frac{1 - e^{-j\gamma_{PO}L}}{j\gamma_{PO}}\right] \quad (17c)$$

and

$$C_1 = \frac{3}{8}\pi \quad (17d)$$

$$C_2 = \frac{3}{8}\pi e^{-jkL[\cos\phi^i - \cos\phi]} \quad (17e)$$

where the various angular terms are given by

$$T_{OP} = 1 - \frac{1}{2}\cos^2\phi^i \quad (18a)$$

$$\gamma_{OP} = k\left[-\cos\phi^i + \cos\phi\right] \quad (18b)$$

$$T_{PO} = 1 - \frac{1}{2}\cos^2\phi^i \quad (19a)$$

$$\gamma_{PO} = k\left[\cos\phi^i - \cos\phi\right]. \quad (19b)$$

The radar cross section of the conducting thin strip scatterer can now be calculated using (13). A similar monostatic radar cross section result is also reported in [13] using elliptic

coordinates where the virtual contour C_v is selected as an elliptic boundary and the thin strip scatterer is simulated by taking the limit as the minor axis of the ellipse tending to zero and the major axis tending to length of the thin strip scatterer. It is interesting to note that the analytical result obtained in this section for the thin strip scatterer also can be verified based on the analytical result of the triangular scatterer, (8)–(12), by substituting the side lengths $L_1 = L_2 = L$, the angles $\delta_1 = 0$ and $\delta_2 = 0$. The z directed induced electric current distribution at any point on the strip is given by

$$J_z(\bar{\rho}') = \{J_{z-}(\bar{\rho}') - J_{z+}(\bar{\rho}')\}\,|_{\text{edge effect}} + J_z(\bar{\rho}')\,|_{\text{corners}}$$

$$\bar{\rho}' \quad \text{on strip.} \tag{20a}$$

Again, the scattered electric field distribution can be viewed as the contribution from the induced electric currents on the thin strip conducting scatterer. It consists of the contribution due to currents on two sides of the smooth edge and the currents due to the two corner effects. As discussed earlier, in the context of presenting a simple and an approximate analytical solution, the corner effects are considered only due to the dominant curvature effect, but the remaining minor contribution [15] due to slope of the radius of curvature is excluded. Using (1), (5b), and (6), the electric current distribution on the thin strip scatterer is calculated as the difference between the induced current on the bottom contour AB and the top contour CD in a limit as ϵ tends to zero, and is given by

$$J_z(\rho')\,|_{\text{edge } OP} = \frac{-j}{\eta k}\left[\frac{\partial E_z^s(\bar{\rho}')}{\partial n'} + \frac{\partial E_z^i(\bar{\rho}')}{\partial n'}\right],$$

$$\bar{\rho}' \quad \text{on } OA_{z-} + OA_{z+}$$

$$= \frac{2E_0}{\eta}\sin\phi^i e^{-jk\rho'\cos\phi^i}. \tag{20b}$$

In (16), the scattered electric field distribution due to the two wedge type corners can be viewed as the contribution due to the electric current distribution which principally exists at the two corners $m = 1$ and 2 of the scatterer in the form of isolated line sources with weighted amplitudes corresponding to the internal wedge angles and the angle of TM incident excitation. Based on (13) and (17a), Fig. 5(a) shows the monostatic radar cross section in decibels for the case of a perfectly conducting thin strip scatterer as a function of monostatic angle $\phi = \pi + \phi^i$. The dimension of the strip scatterer is selected as $kL = 10$ and the angle $\beta_1 = 0$. The OSRC result for the radar cross section shown in the Fig. 5(a) is also compared with the numerical solution obtained based on the electric field integral equation [3]. The electric field integral equation is solved using the method of moments numerical scheme with a resolution of 20 pulse samples for every half-wavelength. Two types of monostatic comparison data are presented in Fig. 5(a). If the two corner effects are excluded, the comparison between OSRC and integral equation monostatic data is poor for certain incident angles. With the two corner effects included, a better comparison is obtained for various excitation angles including broadside and grazing angles of incidence. Similarly, Fig. 5(b) shows comparative result for the bistatic radar cross section in decibels for the same thin strip scatterer with broad side excitation.

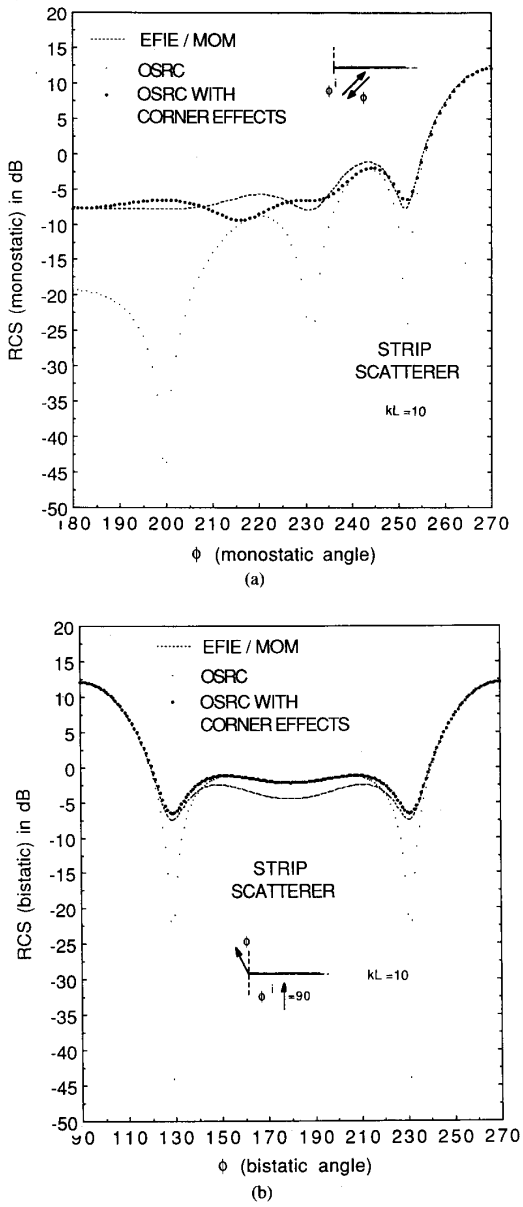

Fig. 5. Monostatic radar cross section of thin strip conducting scatterer using second-order OSRC—TM excitation. (b) Bistatic radar cross section of thin strip conducting scatterer using second-order OSRC—TM excitation, $\phi^i = 90$.

V. Conclusion

With engineering applications in mind, this paper presented a simple and an approximate analytical solution for the analysis of electromagnetic scattering by a perfectly conducting two dimensional object by invoking on-surface radiation condition theory. The close form analytical result for the induced electric current distribution and the radar cross sec-

tion is applicable to the case of a convex conducting object having two dimensional cross section with arbitrary edges and corners. Canonical scattering objects, such as, a triangular shaped scatterer and a thin strip scatterer are analyzed, and numerical data concerning both the monostatic and the bistatic radar cross section for the transverse magnetic excitation are presented with comparison to assess usefulness of the results. Similar study of the two dimensional conducting scatterer is also undertaken for the transverse electric excitation and is reported separately.

ACKNOWLEDGMENT

The authors wish to thank Dr. Arthur Jordan of NRL for helpful discussion during the course of this investigation.

REFERENCES

[1] J. Bowman, T. B. A. Senior, and P. L. E. Uslenghi, *Electromagnetic and Acoustic Scattering by Simple Shapes*. Amsterdam: North Holland, 1969.

[2] A. J. Poggio and E. K. Miller, "Integral equation solutions of three-dimensional scattering problems," *in Computer Techniques for Electromagnetics*, R. Mittra, Ed. Elmsford, NY: Pergamon, 1973.

[3] K. Umashankar, "Numerical analysis of electromagnetic wave scattering and interaction based on frequency-domain integral equation and method of moments techniques," *Wave Motion*, no. 10, pp. 493-525, Dec. 1988.

[4] R. G. Kouyoumijan, "Asymptotic high-frequency methods," *Proc. IEEE*, vol. 53, pp. 864-876, Aug. 1965.

[5] R. C. Hansen, Ed., "Geometric theory of diffraction," Selected Preprint Series, IEEE Press, 1981.

[6] R. G. Kouyoumijan and P. H. Pathak, "A uniform geometrical theory of diffraction of an edge in a perfectly conducting surface," *Proc. IEEE*, vol. 62, pp. 1448-1461, Nov. 1974.

[7] A. Taflove and K. Umashankar, "Review of FD-TD Numerical Modeling of Electromagnetic Wave Scattering and Radar Cross Section," *Proc. IEEE*, Special Issue on Radar Cross Section, vol. 77, pp. 682-699, May 1989.

[8] G. A. Kriegsmann, A Taflove, and K. Umashankar, "A new formulation of electromagnetic wave scattering using an on-surface radiation boundary condition," *IEEE Trans. Antennas Propagat.*, vol. AP-35, pp. 153-161, 1987.

[9] A. Bayliss and E. Turkel, "Radiation boundary conditions for wave-like equations," *Commun. Pure Appl. Math.*, vol. 33, pp. 707-725, 1980.

[10] T. G. Moore, J. G. Blaschak, A. Taflove, and G. A. Kriegsmann, "Theory and application of radiation boundary operators," *IEEE Trans. Antennas Propagat.*, vol. 36, pp. 1797-1812, Dec. 1988.

[11] S. Arendt, K. Umashankar, A. Taflove, and G. A. Kriegsmann, "Extension of on-surface radiation condition theory to scattering by two-dimensional homogeneous dielectric objects," *IEEE Trans. Antennas Propagat.*, vol. 38, pp. 1551-1558, Oct. 1990.

[12] S. Arendt, "Application of the on-surface radiation condition method to two dimensional electromagnetic scattering problems," M.S. thesis, Univ. of Illinois, Chicago, IL, Apr. 1988.

[13] I. D. King, "Application of on-surface radiation condition to electromagnetic scattering by conducting strip," *Electron. Lett.*, vol. 25, no. 1, pp. 56-57, Jan. 1989.

[14] K. Umashankar and W. Chun, "Investigation of the on-surface boundary operators for electromagnetic scattering by conducting object," Tech. Rep. Office of Naval Research (ONR) under Grant N00014-88-K-0475, June 1991.

[15] D. S. Jones, "Surface radiation conditions," *J.I.M.A.*, vol. 41, pp. 21-29, 1988.

Korada Umashankar (S'69-M'75-SM'81), for a photograph and biography please see page 1212 of the August 1991 issue of this TRANSACTIONS.

Wan Chun (S'90) was born in Seoul, Korea. He received the B.S.E.E. degree from Korea University in 1980 and the M.S.E.E. degree from the University of Illinois, Chicago, in 1987, where he is currently working toward the Ph.D. degree.

Since 1987, he has been working as a Research Assistant in the Department of Electrical Engineering and Computer Science. His research interests are in the area of analytical and numerical methods for electromagnetic field scattering and interaction.

Allen Taflove (M'75-SM'84-F'90), for a photograph and biography please see page 906 of the July 1991 issue of this TRANSACTIONS.